JACS
JOURNAL OF THE AMERICAN CHEMICAL SOCIETY
Article
pubs.acs.org/JACS

From Wade–Mingos to Zintl–Klemm at 100 GPa: Binary Compounds of Boron and Lithium

Andreas Hermann,[†] Alexandra McSorley,[†] N. W. Ashcroft,[‡] and Roald Hoffmann*[,†]

[†]Department of Chemistry and Chemical Biology and [‡]Laboratory of Atomic and Solid State Physics, Cornell University, Ithaca, New York 14853, United States

Supporting Information

ABSTRACT: Structural diversity and a variety of bonding schemes emerge as characteristics of the Li–B phase diagram in this ground-state theoretical investigation. We studied stoichiometries ranging from LiB_{15} to Li_5B, over a pressure range from 1 atm to 300 GPa. At P = 1 atm, stability is found for the experimentally known $LiB_{0.8-1.0}$, LiB_3, and Li_3B_{14} phases. As the pressure rises, the latter two structures are no longer even metastable, while the $LiB_{0.8-1.0}$ structures change in geometry and narrow their range of off-stoichiometry, eventually coming at high pressure to a diamondoid NaTl-type LiB. This phase then dominates the convex hull of stability. Other phases emerge as stable points at some pressure: LiB_4, Li_3B_2, Li_2B, and Li_5B. At the boron-rich end, one obtains structures expectedly containing polyhedral motifs, and geometries are governed by Wade–Mingos electron counts; LiB_4 has a $BaAl_4$ structure. In the center and on the lithium-rich side of the phase diagram, Zintl-phase considerations, i.e., bonding between B^{n-} entities, give us insight into the structures—tetrahedral B^- networks in LiB; B pairs to isolated bonds in Li_5B.

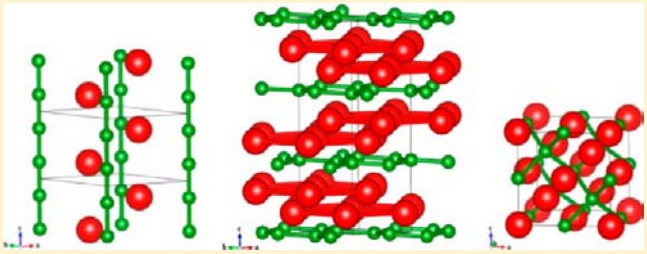

INTRODUCTION

Lithium and boron are two of the lightest elements. In the condensed state, pure lithium appears to be a "simple metal", close to an ideal free electron gas. At room temperature, it crystallizes in a body-centered cubic crystal structure, but at low temperatures, lithium's ground-state structure is the rhombohedral hR9 structure, the structure type of samarium;[1] the very temperature dependence itself indicates the importance of dynamics. Is this a hint that this "simple" metal is not quite that? Under pressure, this suspicion is confirmed: with a significant melting point depression and the appearance of increasingly complicated phases, lithium certainly becomes less "simple" as it is compressed.[2] Lithium is recorded as the 30th superconducting metal; its superconducting transition temperature increases from a mere 0.4 mK at atmospheric pressure by 4 orders of magnitude to about 17 K at P = 35 GPa, close to the phase transition from a face-centered cubic to a cI16 phase.[3]

Boron, on the other hand, has always been recognized as a complex element, both structurally and electronically: its crystalline phases are numerous and inevitably complicated, which is related to its electron deficiency and thus the tendency to form multicenter bonds.[4] Icosahedra and other large polyhedra figure prominently as a structural motif for B. Boron is clearly close to the metal/nonmetal line; it is formally a semiconductor but becomes metallic when doped, for instance with lithium, and can then exhibit superconducting behavior.[5]

So the idea of combining these two elements is intriguing, for they bring very different properties with them and (of course, depending on the actual stoichiometry) the prospect of a wide variety of properties from their compounds. Li and B are not immiscible; the binary phase diagram has been surveyed experimentally, and a variety of phases are stable at low temperatures.[6] Most of these are found on the boron-rich side of the phase diagram, featuring complicated icosahedral boron networks with lithium in interstitial sites. In the remainder of the phase diagram, we find only one known phase, 1:1 in stoichiometry. LiB is interesting since it is not a line phase, for it can incorporate more lithium, with a stability region of up to 55% lithium atomic content.[7]

Here, we present results of extensive computational explorations of the ground state of binary phases of boron and lithium, focusing on our attempt to establish stability regions for various Li_xB_y stoichiometries, these depending on external pressure. Starting from the experimentally known phases at room temperature in the Li–B phase diagram (see Figure 1), we also tried structures for Li_xB_y based on known A_xE_y phase structures, where A and E are heavier elements from groups 1 and 13, respectively. Results from evolutionary structure searches at specific stoichiometries and pressures were also of significant value to us. The technical details of our calculations are given in the Supporting Information (SI) (see also references therein).[2,8−18]

Received: August 27, 2012
Published: October 15, 2012

   dx.doi.org/10.1021/ja308492g | J. Am. Chem. Soc. 2012, 134, 18606–18618

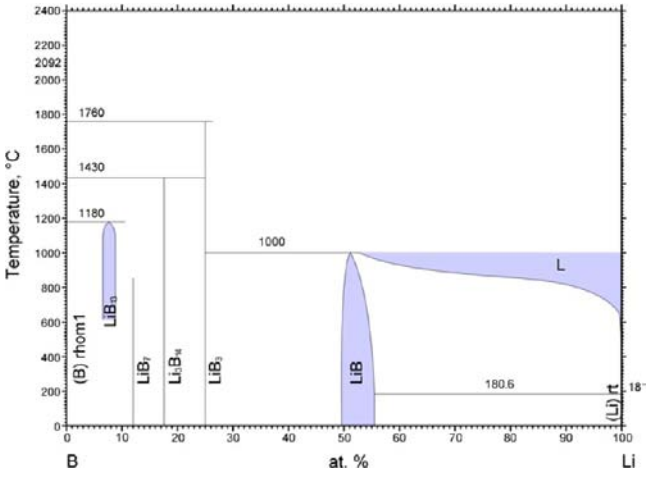

Figure 1. Li−B binary phase diagram. We focus attention here on the low-temperature region. Reprinted with permission of ASM International (www.asminternational.org). All rights reserved.

RESULTS AND DISCUSSION

Computational Phase Diagrams. We begin our study with the phases known at P = 1 atm and room temperature. Of course, just as phases can become unstable under pressure, others can also be stabilized, and hence a better sampling of possible and plausible stoichiometries is eventually necessary. Equally important, pressure-driven phase transitions in known stoichiometries can lower their relative enthalpies.

In Figure 2, we show the relative ground-state enthalpies of formation ΔH_f (with respect to the elemental crystals of Li and B), as obtained from our calculations for all binary Li_xB_y phases. A negative enthalpy of formation indicates that the mixture is more stable than the elements. The *convex hull* of all known ΔH_f values at a given pressure connects the enthalpically stable phases, stable with respect to decomposition into other binaries or the elements. This convex hull is also termed a "tieline" or "global stability line" in the literature. For instance, in Figure 2, at atmospheric pressure, the ground-state enthalpies of all three experimentally known binary phases (Li_3B_{14}, LiB_3, and LiB, to be described in detail momentarily) lie on or close to the computed convex hull and thus these phases are correctly calculated to be stable (the case of LiB is not straightforward, and will be discussed in detail below).

The outcome of our studies is a very rich near-ground-state phase diagram. First and foremost, the experimentally known stoichiometry LiB is very stable even under high pressures. As we will see, the high-pressure LiB structure is quite different from the P = 1 atm one. The slightly more Li-rich phases Li_5B_4 and Li_3B_2 are at least close to enthalpic stability as well. We discuss the properties of these phases, which are close to 1:1 stoichiometry, in great detail in a separate study[19] and summarize the results below.

Li_5B emerges, at medium pressures, as a candidate for a stable ground-state Li−B compound with very high Li content. On the boron-rich side of the phase diagram, the known phases LiB_3 and Li_3B_{14} are not competitive under high pressure; instead, we predict the emergence of a new phase, LiB_4.

The diagrams in Figures 2 and 3 should give a plausible indication of which compositions are candidates for stable Li−B structures at high pressures. In that regard, we note the distinct concentration of stable phases around the midpoint of the binary phase diagram, and also the enthalpy scale: at P = 320 GPa, the 1:1 LiB phase is predicted to be more than 1.5 eV per atom more stable than the elemental crystals, that is, more than 3 eV per formula unit.

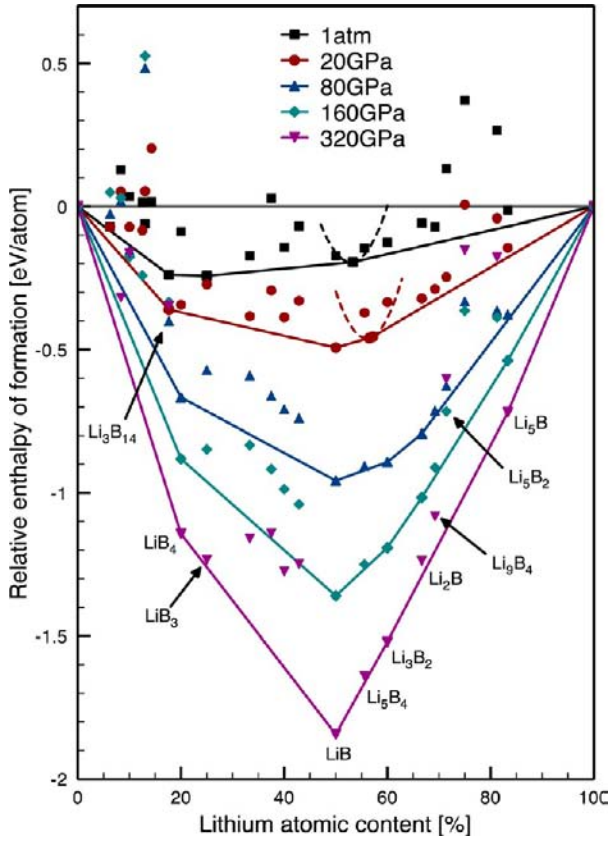

Figure 2. Ground-state enthalpies of formation for Li−B phases, relative to the elemental constituents. Symbols correspond to the enthalpies of individual phases, solid lines are the convex hulls at different pressures, and dashed lines are the parabolic fits to enthalpies for boron-deficient LiB structures (see text). Important stoichiometries are labeled.

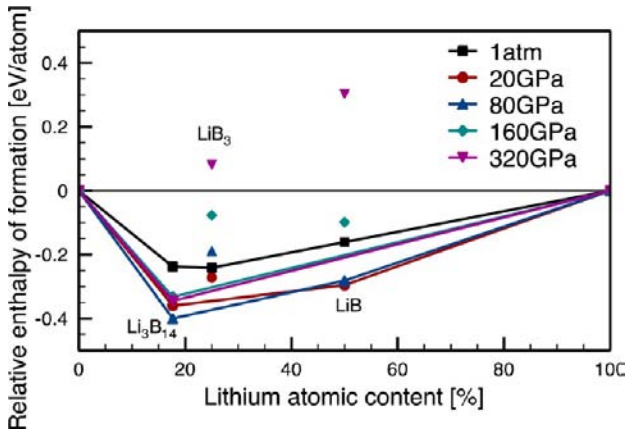

Figure 3. Ground-state enthalpies of formation for experimentally known Li_xB_y phases, shown as a function of Li atomic content, and for various pressures. Enthalpies are relative to the crystalline elements.

Let us now discuss this cornucopia of structures, beginning with the experimentally known stoichiometries at P = 1 atm (and room temperature), then going on to structures which are predicted to be stable at high pressure.

dx.doi.org/10.1021/ja308492g | J. Am. Chem. Soc. 2012, 134, 18606−18618

Experimentally Known Li−B Phases. As shown in Figure 3 above, we find all the known phases LiB, LiB_3, and Li_3B_{14}, to be enthalpically stable at atmospheric pressure in their ground states. If we were to construct a pressure-dependent tieline diagram consisting only of these phases and their ground-state structures, we would obtain Figure 3. We note here that an independent exploration of the Li−B phase diagram in the range of 50−100% Li content has been made by the group of Ma.[20]

Clearly, using only the known structures is an inadequate description of the actual Li−B phase diagram under pressure; for instance, under very high pressure (P = 320 GPa, a volume compression V_0/V = 1.95 for Li_3B_{14}), only Li_3B_{14} seems to form the convex hull (together with elemental B and Li); the LiB_3 and LiB phases are unstable toward decomposition into Li_3B_{14} and Li. The diagram in Figure 3 (and also Figure 2) does not include the experimentally known LiB_7 and LiB_{13} phases: these exhibit huge unit cells and partial occupancies for the Li sites, which makes it difficult to treat them computationally (using even larger supercells as crystalline approximants would be an option, but adequately including configurational entropy terms is more challenging). For this reason, these stoichiometries were also not included in the present study. Below, the experimentally known phases LiB, LiB_3, and Li_3B_{14} are introduced, and the accuracy of our computational approach is verified by comparing the theoretical results to experiment.

LiB_3. This structure crystallizes in a tetragonal structure, space group 127, $P4/mbm$.[21] Boron atoms form a crystal structure of base-centered octahedra which are connected along their corners, and lithium atoms occupy different cavity sites. The boron octahedra are slightly rotated with respect to the lattice vectors (at P = 1 atm, by about 5° in our calculations), and the enthalpy cost to create a more symmetric boron arrangement (toward space group $P4/mmm$) is 15 meV per boron octahedron at P = 1 atm. In an ionic picture, $(Li_2)^{2+}(B_6)^{2-}$ contains stable $(B_6)^{2-}$ units with 20 valence electrons. According to the Wade−Mingos rules on stable cluster electron counts,[22−24] a maximally connected ("closo") polyhedron of n atoms needs $2n$+1 electron pairs to be stable; some of these electrons can be aquired through two-center, two-electron (2c-2e) bonds to other polyhedra, others through electron transfer from available cations. Both take place here: each vertex of the $(B_6)^{2-}$ octahedra is connected to an adjacent octahedron, thus aquiring an additional six electrons that give a total electron count of 26, as expected.

The calculated B−B separations are 1.76−1.78 Å within the octahedra, and 1.72 Å between octahedra, consistent with normal 2c-2e bonding between octahedra, i.e., delocalized electron-deficient bonding between octahedra.[25] The Li^+ ions should be small enough to move relatively freely through the boron lattice, which is hinted at by the partial occupancies of the lithium lattice sites found in experiment, and the fact that ionic conductivity is the dominant charge carrier process above T = 600 K.[21] In our calculations, we assumed the lithium majority sites (Wyckoff site 4*h*, experimental occupancy 0.8) to be completely occupied, and the minority sites (Wyckoff site 4*f*, experimental occupancy 0.2) to be empty (see Figure 4). Both lithium sites are of comparatively low symmetry, i.e., they are not in the center of the boron lattice's cavities; this may be a consequence of the small size of the lithium cations.

The optimized theoretical ground-state crystal structure agrees very well with experimental room temperature data (see Table 1).

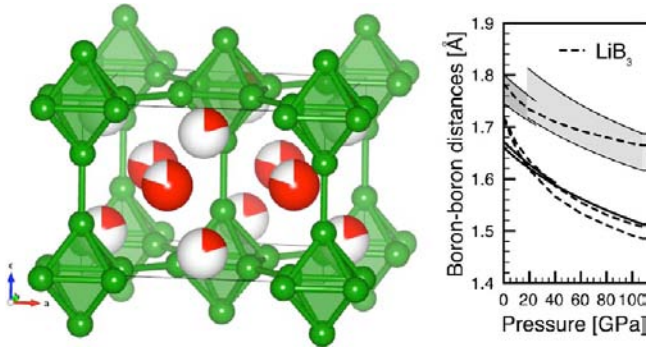

Figure 4. Left: LiB_3 ground-state crystal structure; data from Mair et al.[21] Small green (big red) spheres denote boron (lithium) atoms. Partially filled spheres indicate the partial occupancies of the lithium atom sites. Right: Calculated B−B separations in LiB_3 as a function of pressure (dashed lines), compared to α-boron ($P \leq 20$ GPa) and γ-boron ($P > 20$ GPa), and their inter-icosahedral bonds (solid lines) and intra-icosahedral bonds (shaded areas: there is a range of such bonds in the elemental boron structures).

How do the boron distances compare to other boron structures? In Figure 4, we show the evolution of the shortest B−B separations in LiB_3 as a function of pressure, and compare them to distances in pure α- and γ-boron in their respective pressure ranges of stability. What could be described as a typical 2c-2e bond, the inter-octahedral separation in LiB_3, is in very good alignment with inter-icosahedral bonds in pure boron, and the intra-octahedral separations in LiB_3 fall within the range of the multicenter icosahedral bond lengths of pure boron.

In our DFT calculations, LiB_3 is a semimetal at P = 1 atm, with a vanishing band gap at the Z point. The band structure (apart from the zero band gap) adheres to the cluster electron rules, which predict a gap for the $(B_6)^{2-}$ electron count. The two lowest bands around E = −14 eV are formed by boron 2s orbitals; the 18 other valence bands are bonding combinations of boron 2p orbitals; and the lowest 8 conduction bands are antibonding 2p combinations. The zero band gap is an artifact of the semilocal exchange-correlation functional used in our calculations: using the hybrid HSE06 functional (which includes screened Hartree−Fock exchange)[26] while keeping the geometry fixed results in a band gap of about 0.5 eV at the Z point (see the SI for plots of the band structure). Under pressure, LiB_3 becomes metallic as the bands begin to overlap at the Z point and the electronic density of states (DOS) at the Fermi level increases.

As pressure is increased, the LiB_3 structure changes as well: the boron octahedra rotate around the c axis until their edges are at approximately 45° angles toward the lattice vectors. In the process, each equatorial boron atom becomes connected to *two* neighboring octahedra. If the coordination between octahedra were to be increased, is there a denser octahedral packing available? In the $AuCu_3$ structure type, the Cu-like atoms form corner-fused octahedra, with no inter-octahedral separations. Indeed, we find this structure type (which is also found in $LiAl_3$)[27] more stable than the experimental LiB_3 structure for pressures $P \geq$ 100 GPa.

However, a structure search using evolutionary algorithms (performed with Z = 4 at P = 100 GPa) revealed various other, even more stable structures (see Figure 5). The experimental LiB_3 structure rapidly becomes unstable with respect to these at pressures $P \geq$ 25 GPa. An intermediate stable structure of $P\bar{1}$ symmetry (stable for P = 25−100 GPa) is at very high

dx.doi.org/10.1021/ja308492g | J. Am. Chem. Soc. 2012, 134, 18606−18618

Table 1. Experimental and Theoretical (P = 1 atm) Crystal Structure Parameters of LiB_3

	a [Å]	c [Å]	z_{B1}	x_{B2}	y_{B2}	x_{Li1} (4h)	z_{Li2} (4f)
exptl (T = 300K)[21]	5.975	4.189	0.295	0.138	0.159	0.179	0.147
theory (this work, ground state)	5.982	4.160	0.294	0.135	0.162	0.183	–

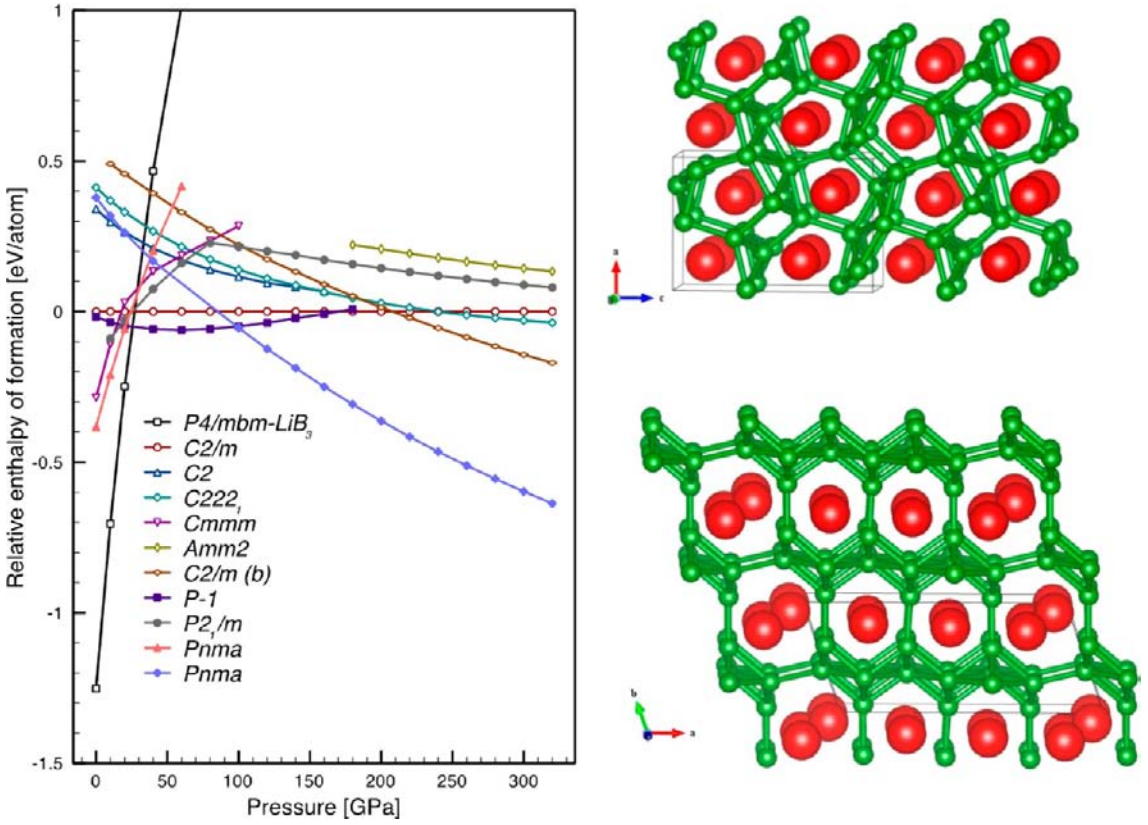

Figure 5. Left: relative ground-state enthalpies of formation for various LiB_3 structures as a function of pressure; all enthalpies are with respect to the $C2/m$ phase. Top right: *Pnma* phase at P = 160 GPa. Bottom right: $P\bar{1}$ phase at P = 100 GPa, with both unit cells indicated by the solid lines.

pressures ($P \geq 100$ GPa) replaced by an orthorhombic phase with space group *Pnma*. The $P\bar{1}$ structure is locally identical to the $BaAl_4$ structure type[28] with Li (B) on the Ba (Al) sites, but, since the stoichiometry is not appropriate, the "layers" of $BaAl_4$ type are separated by B−B linkages and cavities with twice the number of lithium atoms. We are going to see the remarkable $BaAl_4$ structure type again.

The *Pnma* phase, clearly most stable at high pressures, does not recite features of known structure types. It can be characterized as a close-packed polyhedral boron network (three different boron lattice sites have 5, 6, and 7 boron atoms within typical polyhedral bonding distance, respectively) and lithium atoms that occupy cavity channels running along the a axis in Figure 5. Both high-pressure phases are metallic at all pressures.

Li_3B_{14}. This phase has also been found experimentally; it crystallizes in a tetragonal structure, space group 122, $I\bar{4}2d$ (see Figure 6).[29] Here, boron atoms form a complex three-dimensional network of connected B_8 and B_{10} clusters, with lithium atoms occupying cavity sites between these cages, no site occupied by more than 50%. Every lithium site has at least one very close neighbor Li site (d < 1.50 Å), which cannot be simultaneously occupied. For our calculations, we thus chose (arbitrarily) one lithium site to be occupied, and then filled the remaining sites by following the condition that nearest-neighbor lithium sites cannot both be occupied. All lithium sites were treated as equal, even though one of them was measured to be only 20% occupied. Following this procedure, we obtain a unit cell of $I2_12_12_1$ symmetry (space group 24),

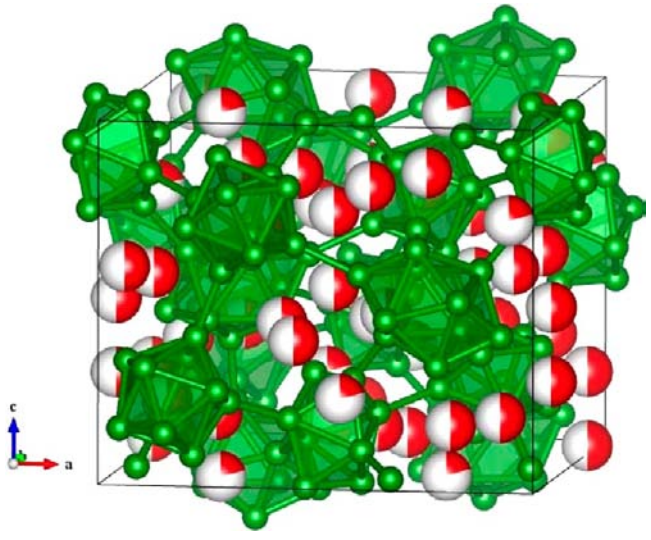

Figure 6. Li_3B_{14} phase, from Mair et al.,[29] with partial Li occupancies indicated (red = occupied fraction).

dx.doi.org/10.1021/ja308492g | J. Am. Chem. Soc. 2012, 134, 18606−18618

which is used in all calculations; all lithium atoms in this cell are more than 2.6 Å apart, which is reasonable.

The optimized unit cell parameters agree very well with experimental data (see Table 2). The atomic positions within the unit cell are equally well described (see the SI). The enthalpy of formation of Li_3B_{14} at P = 1 atm (relative to solid pure boron and lithium) is significant: −32.4 eV per unit cell, or −0.24 eV per atom. Accordingly, Li_3B_{14} is found to be a stable phase in the Li−B phase diagram (see Figure 1). Under pressure, it is even more stabilized compared to the elemental crystals, but ultimately becomes unstable relative to the very stable high-pressure structure of the LiB_4 phase (see further below). At very high pressures, the boron network in Li_3B_{14} collapses anisotropically, leading at the highest pressure studied (P = 320 GPa, volume ratio V/V_0 = 0.51) to short Li−Li distances of d = 1.63 Å. Figure 7 summarizes these structural trends; as a calibration it shows the computed Li−Li separations in elemental Li structures.

Table 2. Experimental and Theoretical Unit Cell Parameters of the Li_3B_{14} Phase

	a [Å]	b [Å]	c [Å]	V [Å^3]
exptl (T = 298 K)	10.764	10.764	8.947	1036.6
theory (this work, ground state)	10.692	10.857	8.962	1040.3

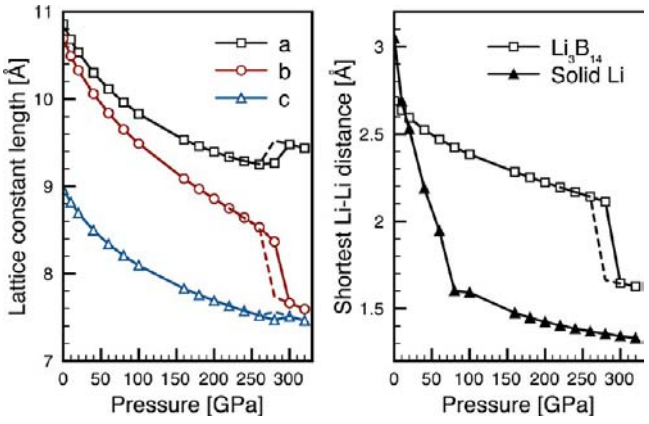

Figure 7. Evolution of lattice constants (left) and shortest Li−Li distances (right) in the experimental structure of Li_3B_{14} under pressure (the Li−Li separations compared to the distances in solid lithium). Solid (dashed) lines are results from ground-state calculations with increasing (decreasing) pressure. The discontinuities are associated with phase transitions.

We find Li_3B_{14} to be semiconducting at P = 1 atm, with a band gap of about 1.4 eV in our calculations. The existence of a band gap is in agreement with the Wade−Mingos rules:[22,30] the unit cell contains 12 "closo" boron clusters (four 8-vertex and eight 10-vertex clusters), the vertices of which are completely connected to adjacent clusters through 2c-2e bonds. Thus, each 8-vertex cluster has 24 valence electrons from its constituent boron atoms, and an additional 8 electrons through the shared bonds with other clusters; it needs 34 valence electrons to reach a stable (Wade−Mingos rules) electron count. Similarly, each 10-vertex cluster has 30 + 10 = 40 electrons available, and needs 42 electrons for its magic electron count. Hence, an additional 24 electrons would be needed per unit cell for stability, and 24 lithium atoms provide these. An increase in pressure does not affect the band gap; only at P > 100 GPa does it begin to decrease and eventually closes.

LiB, and Nearby Compositions. It will be noticed in the literature phase diagram (Figure 1) that the 1:1 composition is not a line phase but represents a region of stability extending toward the lithium-rich side. This is the first clue that this stoichiometry has associated complexities. This suspicion is borne out by the sequence of crystal structure determinations on the structure. These showed a $P6_3/mmc$ space group, with Z = 2.[31,32] The structure may be viewed in a number of ways; perhaps most suggestive from the point of view of facing the problems of the structure is that shown in Figure 8—a simple hexagonal lithium lattice with linear boron chains located in the cavities along the c axis.

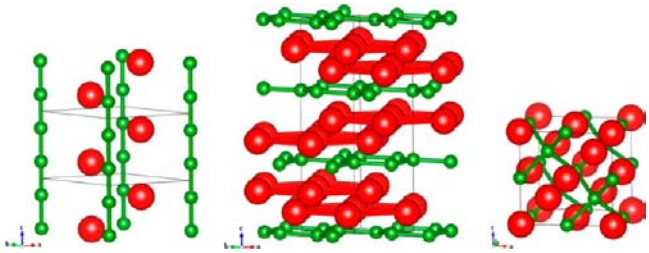

Figure 8. Sequence of crystal structures for 1:1 LiB. From left to right: the experimental structure at P = 1 atm, the proposed ground-state sandwich layer structure at P = 40 GPa, and the NaTl Zintl phase at P = 80 GPa. All structures are drawn to the same scale.

The c axis separation is experimentally 2.798 Å, and that is too short. A word needs to be said about this categorical characterization, made not only by us but by the excellent structural chemists working on this problem.[32,33] If the Li transfers its electrons to B, we have B^-, which is isoelectronic to C. A linear chain allotrope of carbon, called *karbin* or *carbyne*, has been persistently invoked in the literature.[34−37] It (and hence the isoelectronic B chain) can be a cumulenic structure, with all equal B=B bonds, or it could also have alternating single B−B and triple B≡B bonds. A B−B single bond is 1.65−1.80 Å typically, and a triple bond (recently synthesized) is ∼1.56 Å.[38] One way or another, the "experimental" B−B distance, one-half of the c axis, is ∼0.2 Å too short if the stoichiometry is LiB.

The crystallographers studying this structure were faced with a problem of great complexity.[32,33] First it proved impossible to get crystals exactly on stoichiometry; the best study was done on crystals of composition $LiB_{0.885}$. Then they found that the boron chains were disordered and at the same time incommensurate with the lithium matrix; as the temperature was lowered, the boron chains ordered with respect to each other (entropy clearly playing a role here) but remained incommensurate along c with the lithiums.

The most obvious "solution" to the too short BB separation is boron depletion along the chain. Another computational study has explored this, building up a variety of boron-depleted LiB_y structures, showing these to be more stable than pure LiB at atmospheric and moderate pressures (up to P = 30 GPa).[39] In a separate publication, our group together with the group of Bergara has studied the LiB stoichiometry and the region up to 60% Li in some detail.[19] In this section we will only mention the salient features of what we find.

First, if one retains the strict 1:1 stoichiometry, we find (as do other theoretical studies)[40,41] that a $R\bar{3}m$ structure becomes

dx.doi.org/10.1021/ja308492g | J. Am. Chem. Soc. 2012, 134, 18606−18618

more stable. This geometry, called a "metal sandwich" structure in ref 40, is comprised of graphitic layers of B atoms, sandwiched between trigonal nets of Li atoms (see middle of Figure 8).

A structure usually referred to as β-LiB[42] is found to be slightly more stable than α-LiB at atmospheric pressure as well: it differs from α-LiB only through the relative position of the boron chains to the lithium sub-lattice, so that each boron atom is positioned along the c axis between layers of lithium atoms. With increasing pressure, the enthalpy preference of β-LiB over α-LiB is approximately constant, and hence the metal sandwich structures quickly become more stable than both of them as pressure is increased (see Figure 9).

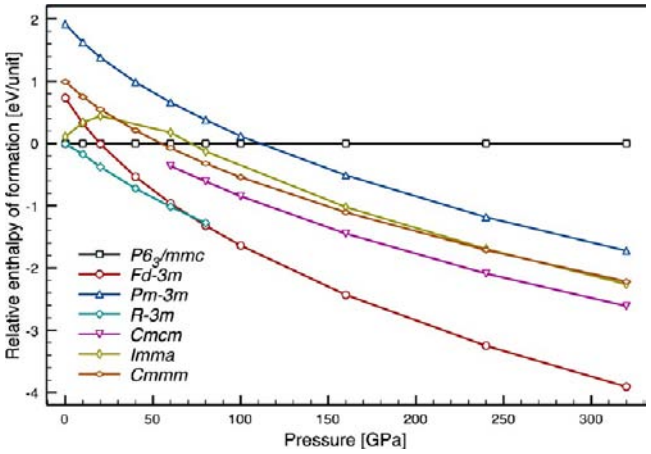

Figure 9. Relative ground-state enthalpies of formation of various LiB phases in the ground state.

At higher pressure, above P = 70 GPa, we find a clear prediction of a NaTl structure type, essentially a diamond network of B^-, with an interpenetrating array of Li^+ ions. This structure is also found in LiAl.[43] Solid-state chemistry invokes a simple and useful concept from Eduard Zintl,[44,45] sometimes called the Zintl–Klemm concept,[46,47] which makes sense of many compounds of groups 13–17. If E is a main-group element and A an alkali metal or alkaline earth element, then not a bad starting point for thinking about the bonding in A_xE_y is to begin by transferring the easily ionized electrons from the x A ions to the main-group elements, followed by bond formation among the E_y anions. The smaller A^+ or A^{2+} cations then can be thought of as fitting into holes in the extended E_y framework. Zintl's prototype structure was NaTl which, if the construct were applied, would be Na^+Tl^-. Tl^- has four valence electrons, so it could form four bonds. And it does—NaTl features relatively short Tl–Tl separations in a diamond lattice of Tl. As one would expect of a "bond-formed" or covalently bound network, such substances usually have a gap between filled and unfilled crystal orbitals. There are exceptions, and the original NaTl is actually a metal.

Note how useful Zintl-type reasoning is here. Chains, hexagonal graphene-like networks, three-dimensional diamondoid structures—B^- runs through all the structures that carbon has or is thought to have (*karbin* is in the latter category). And then it is no surprise that, as the pressure rises, the more dense, higher-coordination networks (diamond over graphene over *karbin*) are favored.

The structural features are mirrored in the electronic DOS of the various structures (see Figure 10): the *karbin* structure

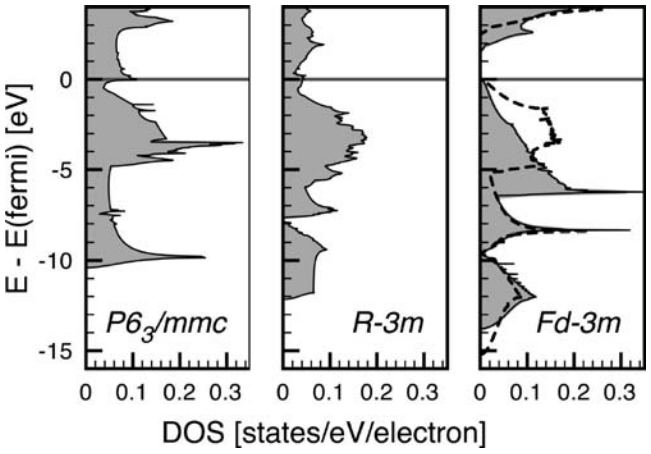

Figure 10. Electronic DOS per valence electron of LiB structures. From left to right: experimental structure at P = 1 atm; the proposed sandwich structure at P = 40 GPa (V/V_0 = 0.62); and the NaTl structure type at P = 80 GPa (V/V_0 = 0.71). Energies are relative to the respective Fermi levels or valence band maximum (VBM). Dashed line in the NaTl structure DOS plot is the DOS for pure diamond, taken at the lattice constant of LiB at P = 80 GPa.

shows the peaked onset of a one-dimensional system, whereas the sandwich structure shows the square onset of a two-dimensional system. Both phases are metallic, but the DOS at the Fermi level is low. For the boron sheets in the sandwich structure, this is where their similarity with graphite (which is a semimetal) ends, although their metallic character is also found in MgB_2. The diamond network has (as one would expect from a classical Zintl compound) a band gap. The last point deserves attention, for our calculations predict that LiB will, under pressure, undergo a metal-to-insulator transition. Relative ground-state enthalpies place this transition at P = 70 GPa. For the NaTl structure, we may also compare the DOS with that of actual diamond, calculated with the same structural parameters as the B sub-lattice in LiB. The general agreement is very good, even though the details show differences (the nuclear charge of C leads to lower energies of the 2s bands, and longer C–C distances than in diamond lead to less dispersive 2p bands than in LiB).

Graphite-like Boron Sheets: From LiB via Li_5B_4 to Li_3B_2. The graphite-like layer structure we discussed above, favored at intermediate pressures for LiB, becomes the source of an *Aufbau* for slightly lithium-rich stoichiometries, for conceptually one can insert lithium layers into that LiB structure, to get, say, (LiBLi)–Li–(LiBLi)–.... This idea works; we find the Li_5B_4 phase with exactly this stacking (known also in the Li–Ga binary system,[48] see Figure 11 for the structure) on or close to the convex hull over the entire pressure range examined. This structure differs greatly from that of a Li_5B_4 phase reported earlier with short-range rhombohedral structure (space group $R3m$, Z = 1, a = 4.93 Å, α = 90°), but with long-range disorder with body-centered cubic symmetry.[49] Perhaps a misassignment occurred; in any case we find the short-range $R3m$ structure to be very unstable indeed. It optimizes to a = 4.87 Å and α = 72.2°, a huge deviation from the pseudo-cubic experimental unit cell.

The 3:2 composition is one extreme of Li intercalation in the layered LiB structure—the B atoms form hexagonal graphite-like sheets, separated by trigonal Li nets, i.e., an (LiBLi)–Li–... stacking. Related Li_3Al_2 crystallizes in space group 166, $R\bar{3}m$.[50]

dx.doi.org/10.1021/ja308492g | J. Am. Chem. Soc. 2012, 134, 18606–18618

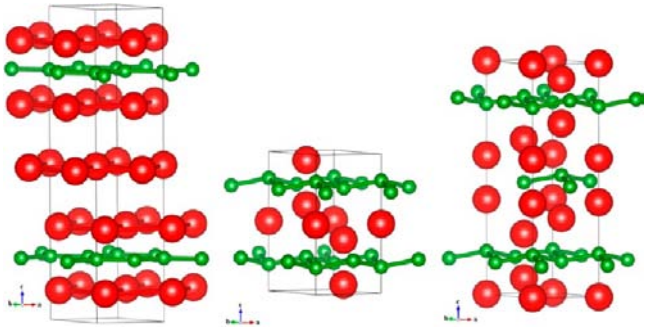

Figure 11. Ground-state structures of Li_5B_4 and Li_3B_2: left, Li_5B_4 at P = 1 atm; middle, Li_5B_4 at P = 80 GPa; right, Li_3B_2 at P = 80 GPa (all drawn on the same length scale).

In our calculations, as the pressure is increased, the boron sheets for all sandwich structures buckle (these structural trends are discussed in detail in the SI; see Figure 11, right side, for the structure). Only for LiB, where sandwich layers are adjacent to each other, does this lead to a three-dimensional boron network, as found in the NaTl structure.

It will be recalled that there is a range of compositions for the nominal LiB phase to the lithium-rich (or boron-poor) side. The reader will see that we have come onto another way of constructing LiB_x structures in this very range, $0.8 \leq x \leq 1$: that is, by changing the number of additional lithium layers, we can, on paper, construct a variety of stoichiometries between LiB and Li_3B_2, including Li_5B_4. Previously, we saw how the same goal could be achieved, by depleting the boron chains in the P = 1 atm structure. The stabilizing feature here is that the B−B distance in the remnant chains approaches a more reasonable value. Kolmogorov and Curtarolo[39] have explored this strategy theoretically, and we have also studied it in detail in our paper on the LiB_x ($0.8 \leq x \leq 1.0$) system.[19] There, we explore in detail the enthalpic consequences of alternative possibilities of moving off 1:1 stoichiometry, by (i) depleting the boron chains in the $P6_3/mmc$ structure, or (ii) intercalating lithium layers into the $R\bar{3}m$ structure.

Both accomplish a stabilization of the lattice, and they do so to a variable degree as a function of pressure. Here is a summary of what we found; for details the reader is referred to our paper, ref 19:

(a) Stabilization by boron chain depletion is effective over a wide pressure range, the optimum atomic ratio shifting to higher lithium atomic content at higher pressure. Enthalpies of formation depend in very good approximation quadratically on the lithium content (these parabolas are part of the phase diagram in Figure 2).
(b) Lithium layer intercalation is stabilizing relative to the elements, but such arrays are metastable with respect to the LiB and Li_3B_2 layer structures.
(c) There is a finite composition range where chain structures are more stable than sandwich structures.
(d) That composition range for boron-depleted chains is reduced in width under pressure, and vanishes above 40 GPa.

A summary of the stability range of the boron-depleted chain structures is shown in Figure 12. The theoretical prediction, that layered structures should be favored under pressure over the boron chain arrangements, has not yet been confirmed in experiment;[51] the vastly different structures might lead to large kinetic barriers.

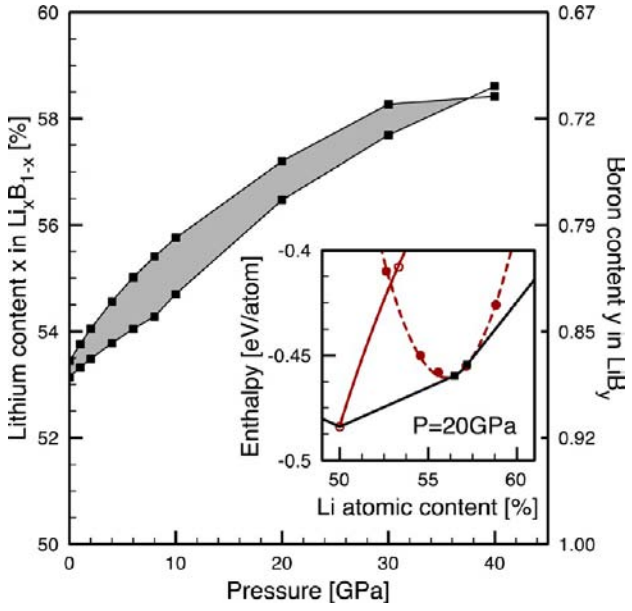

Figure 12. Shaded area is the ground-state stability range of boron-depleted chain structures based on the experimental LiB structure, as a function of pressure. The inset illustrates how the data points in the main figure are obtained: by finding the correct points of the enthalpy parabola, whose tangents are parts of the convex hull of stability.

Other Li−B Stoichiometries. So far, we have concentrated on the stoichiometries that can be found in experiment (or are close, in stoichiometry and their properties). However, a multitude of other phases are found in (presumably chemically similar) other group 1/group 13 binaries, and yet others, completely new, might be stabilized under pressure (we did not investigate possible stabilization of high-temperature phases). As the phase diagram in Figure 2 shows, emergence of new phases is indeed the case, and for the remainder of this paper we will discuss the phases that are, in our calculations, predicted to be stable under certain conditions, but *not yet known* for Li and B.

Boron-Rich Phases: LiB_4. The only new boron-rich phase that we find to be stabilized under pressure in our calculations is LiB_4 (see Figure 2). This stoichiometry is found in various group 1/group 13 binaries ($NaGa_4$, KIn_4, and $RbIn_4$). These structures take on the $D1_3$ or $BaAl_4$ structure type (its ternary variant is $ThCr_2Si_2$), space group $I4/mmm$, with two formula units per unit cell.[28] We already found local features of this structure type in high-pressure phases of the slightly less boron-rich phase LiB_3 (see above). In this structure, the alkali metal is located in the center of truncated rectangular prisms made up by the main-group atoms (see Figure 13). However, as the electronic DOS in Figure 13 reveals, this system is inherently two-dimensional, with the typical square onset at low energies that is characteristic for the two-dimensional electron gas. The structure is thus more aptly described as two-dimensional square layers of boron atoms (denoted as basal borons, B_b), where an additional boron atom (apical boron B_a) caps each $(B_b)_4$ square, and lithium atoms are located in the interstitial region between the boron layers. The boron layers are connected through B_a−B_a bonds.

LiB_4 is a very boron-rich phase, yet the ground state does not feature closed boron polyhedra—unlike the experimental LiB_3 and Li_3B_{14} phases, which are more stable than LiB_4 at low pressures, up to P = 20 GPa. The description of the bonding in

dx.doi.org/10.1021/ja308492g | J. Am. Chem. Soc. 2012, 134, 18606−18618

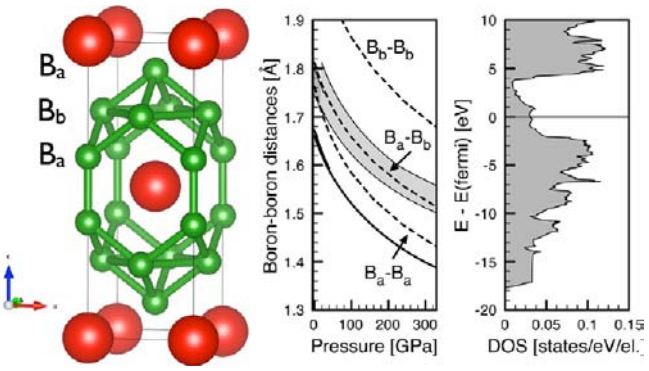

Figure 13. Ground-state LiB_4 phase in the $BaAl_4$ structure type. Left: optimized crystal structure at P = 80 GPa. Middle: B−B separations in LiB_4 (dashed lines) compared to B−B separations in pure boron (solid lines, see also Figure 4). Right: DOS at P = 80 GPa (where V/V_0 = 0.78).

the $BaAl_4$ type, however, relies on the concept of electron-deficient multicenter bonds, here in particular 5c-6e bonds in the $(B_b)_4B_a$ square pyramids.[52] The interlayer B_a−B_a bonds should be 2c-2e bonds, so it is interesting to compare these distances to those of pure boron. This is done in Figure 13: the shortest B−B separations, the B_a−B_a bonds along the *c* axis, are significantly longer than inter-icosahedral 2c-2e bonds in pure boron, and remain such even under high pressure (though they are also significantly more compressible than the usual boron bond); the second shortest B−B separation, the B_a−B_b bond in the square pyramids, is within the range of intra-icosahedral separations found in pure boron; and the B_b−B_b separation in the square pyramids is significantly longer than the other bond types, about 2.07 Å at P = 1 atm, and is shown in Figure 13 as the third shortest B−B separation.

Note that LiB_4 is definitely metallic (and is so at every pressure), even though the Fermi energy falls into a pseudo-gap. The bottom of that pseudo-gap (about 3.5 eV above the Fermi energy at P = 80 GPa) corresponds to a valence electron count of 14 per formula unit—which has been shown to be a point of stability for this structure type.[52,53] Also note that, even though the $BaAl_4$ structure is found in a vast number of various combinations of alkalis, alkaline earths, or rare earths with the triels, our predicted structure seems to be the first that features either lithium or boron as one of the constituents. But it takes external pressure to stabilize it; we cannot comment on the role of temperature regarding its stability.

An alternative to the $BaAl_4$ structure is the $CaMg_2Si_2$ structure where, instead of having each boron square singly capped, every second boron square is doubly capped.[54] This structure type is not competitive for LiB_4, however. Another alternative could be the MgB_4 structure, but it is also not competitive. Further, an evolutionary structure search at P = 80 GPa with Z = 2 also found the $BaAl_4$ structure as the ground state of LiB_4.

One-Dimensional Boron Chains: Li_2B and Li_9B_4. The Li_2B phase was explored by us first in the analogous, existing Li_2Ga structure (prototype $ZrSi_2$), space group 63, *Cmcm*.[49,55] This stoichiometry is also found in Na_2In, which crystallizes in the Na_2Tl structure type, space group $C222_1$;[56] the latter structure is, however, not enthalpically competitive for Li_2B. In the *Cmcm* structure, the B atoms form kinked chains along the *c* axis, and each chain is surrounded by a hexagonal Li tube. In terms of relative lithium atomic content, a transition occurs between this phase and the phases around 1:1 composition described further above, from layered compounds to one-dimensional boron chains within a three-dimensional lithium network. While it is not stable at atmospheric pressure, we find this structure to be stabilized at moderate pressures ($P \geq 20$ GPa), but not at the highest pressures ($P > 160$ GPa) we have studied.

At atmospheric pressure, the boron chains are almost linear (α_{B-B-B} = 152°, see Figure 14), but with increased pressure

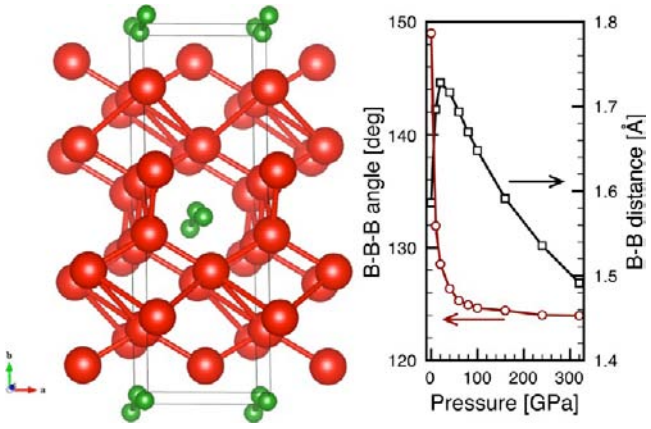

Figure 14. Left: ground-state Li_2B phase at P = 1 atm in the $ZrSi_2$ structure, also found in Li_2Ga. Right: evolution of (i) the shortest B−B distance, and (ii) the B−B−B angle within the kinked chains with pressure.

they become much more pronouncedly kinked. The shortest B−B distance actually *increases* at low pressures, before decreasing monotonously above P = 20 GPa. A large unit cell volume decrease we find at low pressures is hence attributable to the easily compressed lithium sub-lattice.

The electronic structure supports the view of embedded linear boron chains (see Figure 15). The DOS of Li_2B features

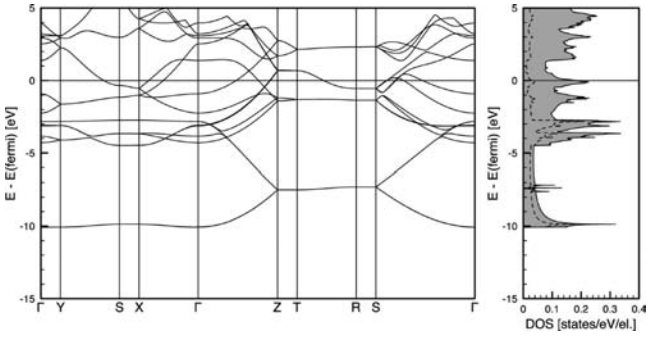

Figure 15. Electronic band structure (left) and DOS (right) of the ground-state *Cmcm* phase of Li_2B, at P = 1 atm. Dashed line in the DOS plot indicates projection onto boron atoms within the atomic pseudo-cutoff radius. Note the large density of states right at the Fermi level.

a very pronounced peak onset, such as that found in one-dimensional electronic systems. The band structure reveals that this peak arises from bands with no dispersion in the *ab* plane, but strong interaction along *c*. These bands are bonding combinations of 2s orbitals of the boron atoms, as an atom-centered projection of the DOS in Figure 15 also shows.

dx.doi.org/10.1021/ja308492g | J. Am. Chem. Soc. 2012, 134, 18606−18618

The Li_9B_4 structure's prototype in our calculations is Li_9Al_4,[57] space group 12, $C2/m$. The boron atoms, as in the Li_2B structure described above, form one-dimensional zigzag chains through the lithium network. The latter, having to accommodate more lithium atoms per boron atom, form pentagonal tubes around the boron chains. However, the shortest Li−B distances are not much longer than the shortest B−B distances (d_{Li-B} = 2.25 Å, d_{B-B} = 1.58 Å), so the boron atoms are effectively close-packed; each has 9 or 10 neighbors (two borons and seven or eight lithiums, respectively), as the coordination polyhedra in Figure 16 show. At P = 1 atm, this phase is very unstable, but it becomes stabilized at intermediate pressures, similar to Li_2B above.

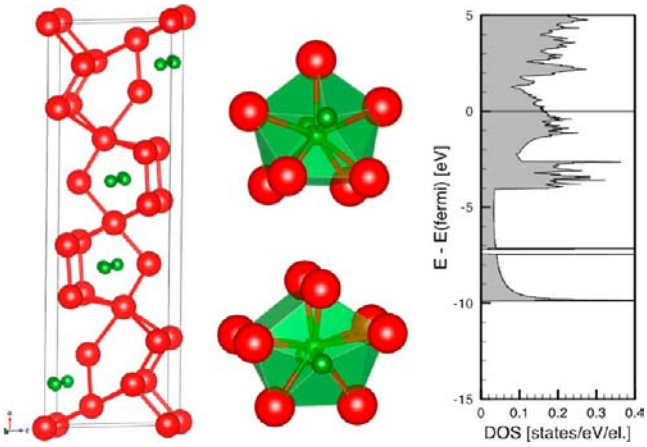

Figure 16. Left: ground-state Li_9B_4 phase, in the Li_9Al_4 structure. Optimized structure at P = 1 atm is shown, with B−B separations ≤2 Å and Li−Li separations ≤3.2 Å drawn as connected. Middle: the coordination polyhedra of the boron atoms, with separations ≤2.7 Å drawn as connected. Right: the electronic DOS at P = 1 atm, exhibiting a rather large DOS at the Fermi level.

Structurally, Li_9B_4 shows behavior very similar to that of Li_2B above. Concentrating on the boron chain feature, we find the chains to be not far from linear at atmospheric pressure (α_{B-B-B} = 150°, see Figure 16), but increasingly bent under pressure. Also, while the unit cell volume rapidly decreases at low pressures, the intrachain B−B distance actually *increases*; again, this is attributable to the compressibility of the lithium sublattice, which enables the boron atoms to rearrange under pressure and keep relatively large distances from each other. The metastability of this and the Li_2B phase at very high pressures can then be explained as further compression of the boron chains (which must happen once the lithium sub-lattice is squeezed tight) is unfavorable.

Note that for neither the Li_2B nor the Li_9B_4 phase were independent structure searches performed. However, in an exchange of information with Prof. Ma, we learned that a structure search performed in his group for Li_2B structures resulted in the Li_2Ga structure as the best candidate structure.[20] It is then not unreasonable to assume that the Li_9Al_4 structure, with very similar features, is also competitive and close to the global minimum for Li_9B_4.

One might be tempted by the success of the Zintl−Klemm perspective for LiB to also try it for Li_2B. Boron would then be considered as B^{2-}, isoelectronic to N or other group 15 elements. We did look for three-connected network structures of boron such as those of P, As, and Sb, into which Li^+ ions were inserted. None proved competitive. The Li_9B_4 structure of Figure 16 incorporates structural elements of the lovely Hittorf violet phosphorus structure,[58] but is different in detail; it is the Li sub-lattice that is phosphorus-like.

Electronically, Li_9B_4 is very similar to Li_2B: the one-dimensional boron chains give rise to a sharp peak at the bottom of the valence DOS (Figure 16).

Li_5B: Boron Pairs and Atoms. Li_5B could also be seen as an extreme Zintl compound, enabling boron to fulfill its electronic octet through electron donation from no less than five lithium atoms. We have not found this composition as a solid in any group 1/group 13 combination, but AB_5 metal alloys are known,[59] and Li_5B is a particularly stable cluster in the Li_nB series.[60] We therefore compared the enthalpies of formation of Li_5B for a variety of intermetallic AB_5 structures, and also performed an evolutionary structure search at P = 60 GPa.

The known AB_5 intermetallic structures have atom type "A" always isolated in a matrix (of varying connectivity) of atoms of type "B". We found the *Cmcm* structure (prototype $BaZn_5$, see Figure 17) to be the most stable of the common structures, becoming enthalpically stable with respect to elemental B and Li above P = 20 GPa.

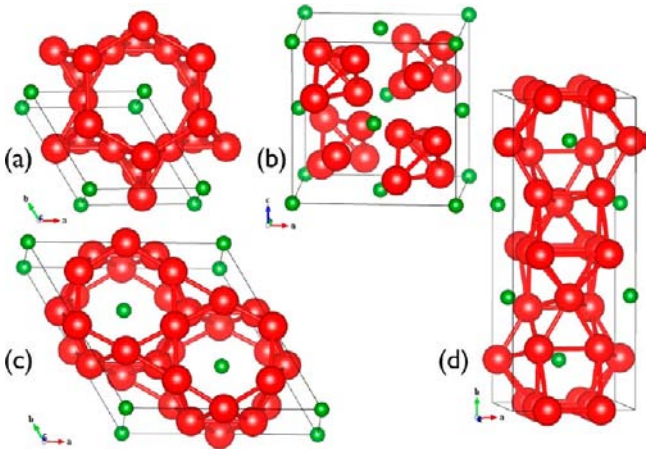

Figure 17. Common ground-state AB_5 structures in intermetallic compounds: (a) $P6/mmm$ ($CaCu_5$); (b) $F\bar{4}3m$ ($AuBe_5$); (c) $P6/mmm$ (YNi_2Al_3); and (d) $Cmcm$ ($BaZn_5$). Li atoms are red, B atoms are green.

In our structure search, however, we found a more stable $P\bar{1}$ structure which features B_2 dimers embedded in a Li matrix, and a $P2_1/m$ structure which features kinked B chains embedded in a different Li matrix, where each B chain is surrounded by a hexagonal tube of Li atoms (the difference with the Li_2B phase described above being that adjacent lithium tubes in Li_5B do not share vertices). Both structures are more stable than those of the common metallic phases (see Figure 18) and could be stable at high pressures. At pressures $P \geq 100$ GPa, an orthorhombic phase of *Immm* symmetry, its monoclinic distortion of $C2/m$ symmetry, and another orthorhombic phase of *Cmma* symmetry are more stable than the $P2_1/m$ structure. The *Immm* and $C2/m$ phases are similar to the $P\bar{1}$ structure, with B_2 dimers surrounded by a lithium cage, as shown in Figure 19. The *Cmma* phase, which we find most stable for $P \geq 90$ GPa, has individual boron *atoms* surrounded by lithium cages. We note that a structure of *Cmcm* symmetry, found by Ma and co-workers,[20] is slightly more stable than the

dx.doi.org/10.1021/ja308492g | J. Am. Chem. Soc. 2012, 134, 18606−18618

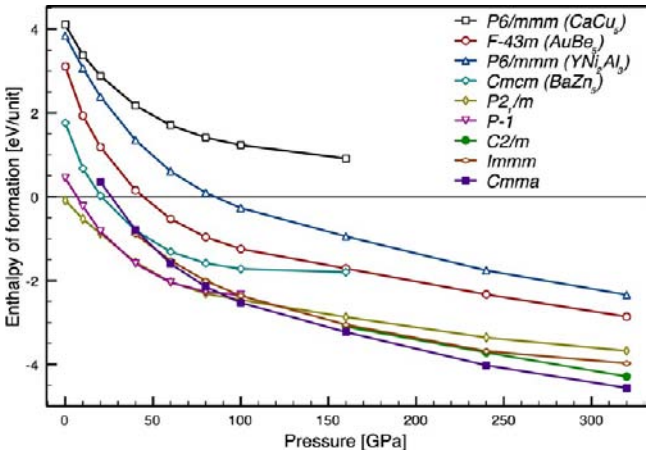

Figure 18. Relative ground-state enthalpies of formation per Li_5B unit, normalized to elemental B and Li crystals.

Cmma phase (about 40 meV per formula unit) in the pressure range 90 GPa $\leq P \leq$ 110 GPa.

Are there really B_2 dimers in the *Imm*2 and *C*2/*m* structures? At P = 20 GPa, the lowest pressure at which we could stabilize the *Immm* structure, the B−B separation is 1.68 Å. It then *increases* as pressure is increased, up to 1.90 Å at P = 80 GPa, after which it monotonically decreases down to 1.67 Å at P = 320 GPa. All these distances are in line with what could be expected for boron dimers. The initial bond length increase is not what one expects of simple confinement, yet it is consistent with the idea that the initial squeezing of the lithium sub-lattice brings more electrons into the B−B bond, which occupy crystal orbitals that are locally B−B antibonding and thus lengthen the bond.[61]

The favored structures are clearly *not* simple Zintl compounds. In the best low-pressure structure, only some of the lithium atoms interact with boron in an electron donation/acceptance process, forming sub-lattices similar to the Li_2B structure discussed above, with kinked boron chains in hexagonal lithium tubes. The remaining lithium atoms fill interstitial space; this should be possible also for higher lithium atomic content, thus creating a "solvation" environment for boron chains in lithium-rich compounds. At high pressures, we find stable cage structures, which is a common theme in AB_5 intermetallics structures, but here with both B_2 units and single atoms at the centers of the cages.

In our information exchange with Prof. Ma, we learned about their results on Li_6B, an even more lithium-rich phase.[20] This phase then features single B atoms in a lithium cage structure; it is stable at pressures $P \geq$ 80 GPa. We cannot rule out that more interesting phases can be stabilized at the lithium-rich end of the Li−B phase diagram.

Interstitial Electron Density in Li_5B. An intriguing feature of the structures with B_2 units is the localization of electronic charge in interstitial space: in Figure 20, we show isosurfaces of the electron localization function (ELF[62]), which clearly show pronounced maxima in the region *between* the B−Li cages (isosurface value is 0.85), for both the *Immm* and *C*2/*m* structures. It has been noticed before that ELF localization in interstitial space could hint at missing impurity atoms,[63] but in this case the "vacancy" sites are probably too small to allow for an additional atom; also, the DOS of these structures (not shown here) does not exhibit a gap or pseudo-gap at a specific higher electron count, which would favor incorporation of additional atoms into the structural framework. The charge density (bottom of Figure 20) also has local maxima in the interstitial regions. The shortest Li−Li separations at $P \geq$ 160 GPa are slightly shorter than in Li metal at the corresponding pressures.

As we see, the lithium network incorporates both localized B_2 units and localized electrons, forming a binary alloy electride. The (at high pressures) slightly more stable *Cmma* structure, however, does not show signs of interstitial electron localization. The interstitial charge localization is fascinating and will be explored further elsewhere.

We note that this is the first time in the exploration of the Li/Be/B binary and ternary phases that we have found valence

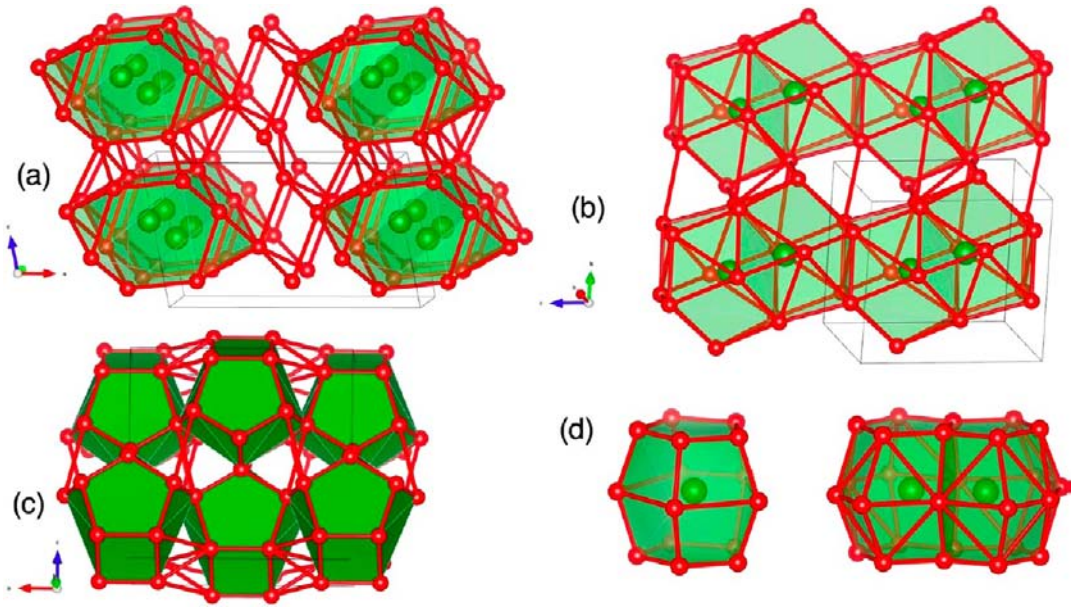

Figure 19. (a) Ground-state $P2_1/m$ structure for Li_5B and (b) $P\bar{1}$ structure, both at P = 60 GPa. (c) *Cmma* structure at P = 160 GPa. (d) Boron atom and dimer cages found in the high-pressure phases of Li_5B.

dx.doi.org/10.1021/ja308492g | J. Am. Chem. Soc. 2012, 134, 18606−18618

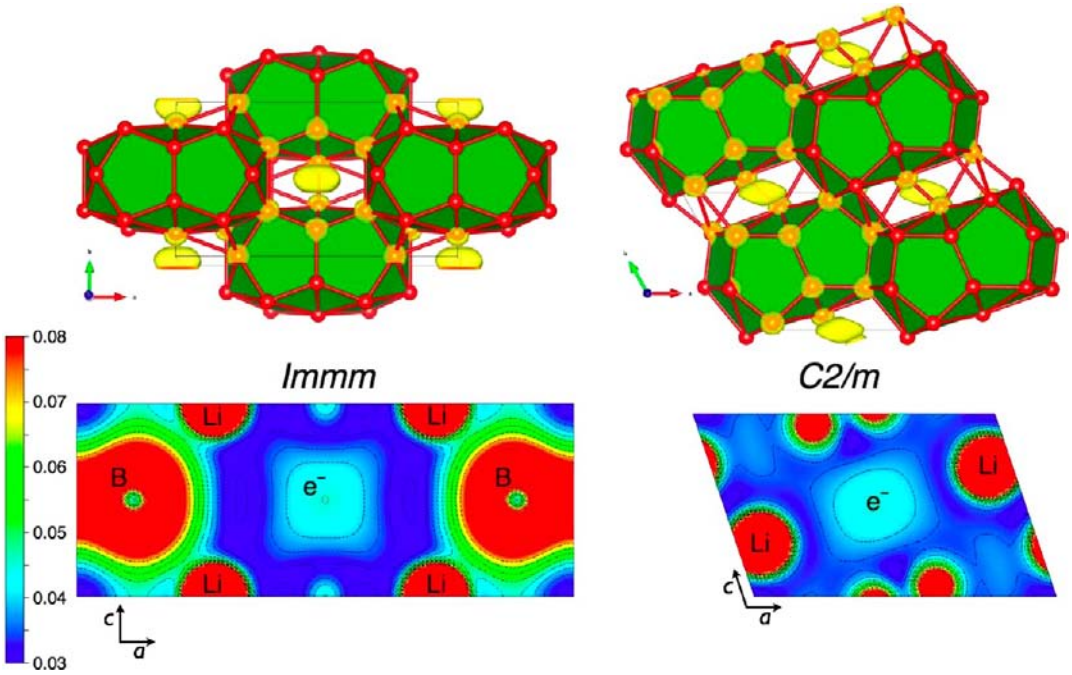

Figure 20. Top: *Immm* (left) and *C*2/*m* (right) structures of Li_5B at P = 160 GPa, both with ELF isosurfaces (ELF = 0.85). Bottom: corresponding electronic charge density profiles, both for cuts along the [010] direction. Units are e/Å^3.

electron density away from the atoms—a feature of dense structures found first in the high-pressure Cs^{IV} phase of cesium,[64,65] later predicted for pure lithium by Neaton and Ashcroft,[66] and since found in several other theoretical studies of high-pressure elemental structure.[67,68]

Metastable Stoichiometries. We examined a variety of other stoichiometries, but did not find these to be competitive at any pressure. Below is a short summary of those we surveyed, ones that at least reach metastability—defined here quite arbitrarily as having an enthalpy of formation within 100 meV/atom of the convex hull. Structural information and figures of these phases can be found in the SI.

Between 25% and 50% Lithium Atomic Content. There is a curious void in the Li−B phase diagram between 25% and 50% lithium content. No phases are known between LiB_3 and LiB, and almost none in the other group 1/group 13 binary systems. The only exceptions are the phases K_2Ga_3, Rb_2In_3, and Cs_2In_3, all of which crystallize in the same structure type (featuring connected layers of octahedra of the boron group element), in space group $I4/mmm$.[69,70] Might pressure stabilize these or other stoichiometries in this region of the Li−B phase diagram?

We performed ground-state structure searches at a pressure of P = 80 GPa for the phases Li_3B_5, Li_2B_3, and Li_3B_4, all with Z = 2, and at P = 1 atm for LiB_2 with Z = 4. At atmospheric pressure, none of our structural candidates for the Li_2B_3 phase is more stable than the K_2Ga_3 structure, but at pressures of P = 20 GPa and higher, a succession of other structures is stabilized. However, as the phase diagram in Figure 2 shows, none of these structures in this or the other phases is enthalpically stable, even at very high pressures, where all of them would decompose into the LiB and LiB_4 phases. Only the Li_2B_3 and LiB_2 structures can be deemed "metastable", and only at pressures $P \leq 40$ GPa. The high-pressure phase of LiB_2 is found to be the AlB_2 structure type (see the SI for details). We cannot exclude that one or several of these phases could be stabilized at high temperatures.

Li_5B_2. This is the Li_5Tl_2 structure (also Li_5Sn_2), space group 166, $R\bar{3}m$.[71] In a hexagonal unit cell, this structure comprises chains of five lithium atoms alternating with B_2 dimers along the c axis. We find this structure to be close to stability at intermediate pressures (20 GPa $\leq P \leq$ 80 GPa).

$Li_{13}B_3$. This quite unusual stoichiometry, found in the Li−In system,[72] crystallizes there in a very symmetric structure (cubic symmetry, space group $Fd\bar{3}m$): in a supercell of a body-centered cubic lithium crystal, 3 out of every 16 lithium atoms are replaced by boron, such that the boron sub-lattice consists of corner-sharing tetrahedra. In the Li−B system, this phase is only metastable at intermediate pressures, 40 GPa $\leq P \leq$ 80 GPa.

LiB_{15}. This stoichiometry is found in the Na−B system, and its structure is orthorhombic, space group *Imma*.[73] It consists mainly of B_{12} icosahedra, and three additional interstitial borons per alkali atom. These three borons form an obtuse triangle that connects a total of six B_{12} icosahedra. This phase is only metastable at low pressures, up to about P = 50 GPa. We did not find any of the other known very boron-rich binary phases (i.e., those where boron forms icosahedral clusters) to be close to the convex hull in the Li−B system.

■ CONCLUSIONS

We have presented a comprehensive computational survey of possible stable phases in the Li−B binary system under pressure. Binary phases of lithium and boron are significantly stabilized by pressure, new phases emerge, and known phases undergo phase transitions to close-packed structures. The latter effect is epitomized by the 1:1 LiB phase, where we find a progression in the boron sub-lattice from one-dimensional chains, via two-dimensional sheets, to a three-dimensional diamondoid network, as pressure increases. For other phases, external pressure often stabilizes structure types that occur in

dx.doi.org/10.1021/ja308492g | J. Am. Chem. Soc. 2012, 134, 18606−18618

other group 1/group 13 binaries of heavier, larger atoms; this is the case for various lithium-rich phases.

In Figure 21, we summarize the stability ranges for the various Li−B phases that we find stable or at least close to

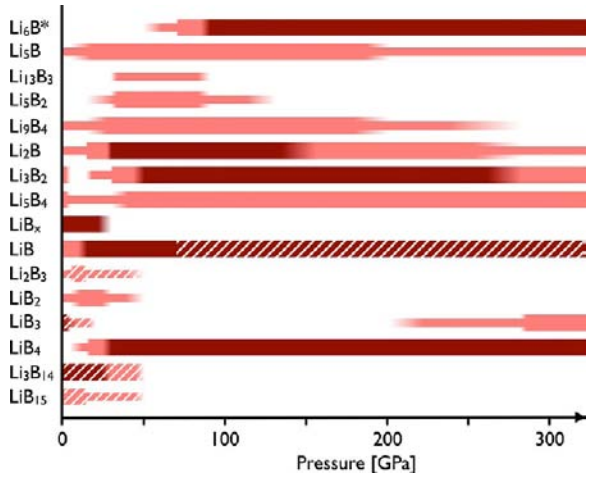

Figure 21. Ground-state binary phase stability ranges as a function of pressure. Dark red (light red, thin light red) lines denote, respectively, stable structures, structures within 50 meV/atom of stability, and structures within 100 meV/atom of stability. LiB_x refers to compositions with $0.8 \leq x \leq 1.0$. Structures that we find nonmetallic are indicated by striped patterns. *The Li_6B structure is the one kindly given to us by Prof. Ma.

stability. Note that these are ground-state enthalpies, and hence dynamical contributions to the Gibbs free energy at finite temperatures (or zero-point motion effects) are not considered here. Most of the stable binary phases we find are metallic (some feature a quite high DOS at the Fermi level). Exceptions are most of the boron-rich phases (except for LiB_4), and the high-pressure phase of LiB.

The Zintl−Klemm concept proves very useful to understand some of these structures, especially the 1:1 compound LiB. Our calculations predict that the finite stability range found for LiB_x ($0.8 \leq x \leq 1.0$) vanishes at pressures higher than 40 GPa; the reason is the emergence of more-stable structures with two-dimensional boron sheets and a variable density of intercalated lithium layers. As we look at compounds with higher lithium content, we find one-dimensional boron chains (around Li_2B), and finally isolated boron dimers (metastable in Li_5B_2, stable in Li_5B) in a lithium matrix. On the boron-rich side, the known phases LiB_3 and Li_3B_{14} quickly become unstable with respect to LiB_4 which, in the well-known $BaAl_4$ structure, dominates the Li_yB ($y < 1.0$) composition range of the Li−B phase diagram. Curiously, we do not find any stable phases between 25% and 50% lithium content, only a couple of metastable phases at low pressures. On either side of this region, different rules govern the formation of stable structures: for more boron-rich compounds, boron cluster formation following the Wade−Mingos electron counts, and the Zintl−Klemm concept for more lithium-rich compounds. In between, immiscibility seems to prevail.

Having established the energetics and stability of the various Li−B phases, we plan to study some of their electronic properties in more detail. For instance, the presence of essentially layered structures on the lithium-rich side of the phase diagram, with quite large DOS values at the Fermi level, is intriguing, and investigating the electron−phonon coupling in these structures should be insightful. The emergence of the LiB_4 phase as a boron-rich material without "closo" boron polyhedra is also interesting and warrants further investigation, as does the electron density of the Li atoms in the high-pressure Li_5B phase.

■ ASSOCIATED CONTENT

Supporting Information

Details on computational methods used, crystal structures, analysis of structural and electronic features, and additional figures. This material is available free of charge via the Internet at http://pubs.acs.org.

■ AUTHOR INFORMATION

Corresponding Author

rh34@cornell.edu

Notes

The authors declare no competing financial interest.

■ ACKNOWLEDGMENTS

We thank Aitor Bergara and Yanming Ma for generous exchange of information on various parts of the Li−B phase diagram. Support for our work comes solely from EFree, an Energy Frontier Research Center funded by the U.S. Department of Energy (Award No. DESC0001057 at Cornell). Computational resources provided by the Cornell NanoScale Facility (supported by the National Science Foundation through grant ECS-0335765) and by the XSEDE network (provided by the National Center for Supercomputer Applications through grant TG-DMR060055N) are gratefully acknowledged.

■ REFERENCES

(1) Overhauser, A. W. *Phys. Rev. Lett.* **1984**, *53*, 64−65.
(2) Guillaume, C. L.; Gregoryanz, E.; Degtyareva, O.; McMahon, M. I.; Hanfland, M.; Evans, S.; Guthrie, M.; Sinogeikin, S. V.; Mao, H.-K. *Nature Phys.* **2011**, *7*, 211.
(3) Deemyad, S.; Schilling, J. *Phys. Rev. Lett.* **2003**, *91*, 167001.
(4) Greenwood, N. N.; Earnshaw, A. *Chemistry of the Elements*; Butterworth-Heinemann: Oxford, 1998; pp 139−215.
(5) Nagatochi, T.; Hyodo, H.; Sumiyoshi, A.; Soga, K.; Sato, Y.; Terauchi, M.; Esaka, F.; Kimura, K. *Phys. Rev. B* **2011**, *83*, 184507.
(6) Villars, P.; Okamoto, H.; Cenzual, K. *ASM Alloy Phase Diagrams Center*; ASM International: Materials Park, OH, 2006.
(7) Borgstedt, H. B.; Guminski, C. *J. Phase Equilib.* **2003**, *24*, 572−574.
(8) Blöchl, P. E. *Phys. Rev. B* **1994**, *50*, 17953−17979.
(9) Hanfland, M.; Syassen, K.; Christensen, N. E.; Novikov, D. L. *Nature* **2000**, *408*, 174−178.
(10) Kresse, G.; Furthmüller, J. *Phys. Rev. B* **1996**, *54*, 11169−11186.
(11) Kresse, G.; Joubert, D. *Phys. Rev. B* **1999**, *59*, 1758−1775.
(12) Lonie, D. C.; Zurek, E. *Comput. Phys. Commun.* **2011**, *182*, 372.
(13) Marqués, M.; McMahon, M. I.; Gregoryanz, E.; Hanfland, M.; Guillaume, C. L.; Pickard, C. J.; Ackland, G. J.; Nelmes, R. J. *Phys. Rev. Lett.* **2011**, *106*, 095502.
(14) Mondal, S.; van Smaalen, S.; Schönleber, A.; Filinchuk, Y.; Chernyshov, D.; Simak, S.; Mikhaylushkin, A.; Abrikosov, I.; Zarechnaya, E.; Dubrovinsky, L.; Dubrovinskaia, N. *Phys. Rev. Lett.* **2011**, *106*, 215502.
(15) Oganov, A. R.; Chen, J.; Gatti, C.; Ma, Y.; Ma, Y.; Glass, C. W.; Liu, Z.; Yu, T.; Kurakevych, O. O.; Solozhenko, V. L. *Nature* **2009**, *457*, 863−867.
(16) Perdew, J. P.; Burke, K.; Ernzerhof, M. *Phys. Rev. Lett.* **1996**, *77*, 3865−3868.

(17) Rousseau, B.; Xie, Y.; Ma, Y.; Bergara, A. *Eur. Phys. J. B* **2011**, *81*, 1−14.
(18) Zarechnaya, E. Y.; Dubrovinsky, L.; Dubrovinskaia, N.; Filinchuk, Y.; Chernyshov, D.; Dmitriev, V.; Miyajima, N.; El Goresy, A.; Braun, H. F.; Van Smaalen, S.; Kantor, I.; Kantor, A.; Prakapenka, V.; Hanfland, M.; Mikhaylushkin, A. S.; Abrikosov, I. A.; Simak, S. I. *Phys. Rev. Lett.* **2009**, *102*, 185501.
(19) Hermann, A.; Suarez-Alcubilla, A.; Gurtubay, I. G.; Yang, L.-M.; Bergara, A.; Ashcroft, N. W.; Hoffmann, R. *Phys. Rev. B* **2012**, *86*, 144110.
(20) Peng, F.; Miao, M.-S.; Wang, H.; Li, Q.; Ma, Y. *J. Am. Chem. Soc.* **2012**, DOI: 10.1021/ja308490a.
(21) Mair, G.; von Schnering, H. G.; Wörle, M.; Nesper, R. *Z. Anorg. Allg. Chem.* **1999**, *625*, 1207−1211.
(22) Wade, K. *J. Chem. Soc. D: Chem. Commun.* **1971**, 792.
(23) Mingos, D. M. P. *Nature Phys. Sci.* **1972**, *236*, 99−102.
(24) Fehlner, T. P.; Halet, J.-F.; Saillard, J.-Y. *Molecular Clusters*; Cambridge University Press: Cambridge, UK, 2007; p 378.
(25) *Boron Hydride Chemistry*; Muetterties, E. L., Ed.; Academic Press Inc.: San Diego, CA, 1975; p 532.
(26) Heyd, J.; Scuseria, G. E.; Ernzerhof, M. *J. Chem. Phys.* **2003**, *118*, 8207−8215.
(27) Yoshi-yama, T.; Hasebe, K.; Mannami, M. *J. Phys. Soc. Jpn.* **1968**, *25*, 908.
(28) Bruzzone, G. *Acta Crystallogr. B* **1969**, *25*, 1206−1207.
(29) Mair, G.; Nesper, R.; von Schnering, H. G. *J. Solid State Chem.* **1988**, *75*, 30−40.
(30) Prasad, D. L. V. K.; Balakrishnarajan, M. M.; Jemmis, E. D. *Phys. Rev. B* **2005**, *72*, 195102.
(31) Liu, Z.; Qu, X.; Huang, B.; Li, Z. *J. Alloys Compd.* **2000**, *311*, 256−264.
(32) Wörle, M.; Nesper, R. *Angew. Chem., Int. Ed.* **2000**, *39*, 2349−2353.
(33) Wörle, M.; Nesper, R.; Chatterji, T. K. *Z. Anorg. Allg. Chem.* **2006**, *632*, 1737−1742.
(34) Kasatochkin, V. I.; Sladkov, A. M.; Kudryavtsev, Y. P.; Popov, N. M.; Korshak, V. V. *Dokl. Chem.* **1967**, *177*, 1031.
(35) Smith, P. P. K.; Buseck, P. R. *Science* **1982**, *216*, 984−986.
(36) Whittaker, A. G. *Science* **1978**, *200*, 763−764.
(37) Chalifoux, W. A.; Tykwinski, R. R. *Nature Chem.* **2010**, *2*, 967−971.
(38) Braunschweig, H.; Dewhurst, R. D.; Hammond, K.; Mies, J.; Radacki, K.; Vargas, A. *Science* **2012**, *336*, 1420−1422.
(39) Kolmogorov, A. N.; Curtarolo, S. *Phys. Rev. B* **2006**, *74*, 224507.
(40) Kolmogorov, A. N.; Curtarolo, S. *Phys. Rev. B* **2006**, *73*, 180501.
(41) Calandra, M.; Kolmogorov, A. N.; Curtarolo, S. *Phys. Rev. B* **2007**, *75*, 144506.
(42) Rosner, H.; Pickett, W. E. *Phys. Rev. B* **2003**, *67*, 054104.
(43) Kishio, K.; Brittain, J. O. *J. Phys. Chem. Sol.* **1979**, *40*, 933.
(44) Zintl, E. *Angew. Chem.* **1939**, *52*, 1−6.
(45) *Chemistry, structure, and bonding of Zintl phases and ions*; Kauzlarich, S. M., Ed.; VCH: New York, 1996.
(46) Klemm, W. *Proc. Chem. Soc.* **1958**, 329.
(47) Nesper, R. *Prog. Solid State Chem.* **1990**, *20*, 1−45.
(48) Stöhr, J.; Schäfer, H. *Z. Anorg. Allg. Chem.* **1981**, *474*, 221−225.
(49) Wang, F. E.; Mitchell, M. A.; Sutula, R. A.; Holden, J. R.; Bennett, L. H. *J. Less-Common Metals* **1978**, *61*, 237−251.
(50) Tebbe, K.-F.; Von Schnering, H. G.; Rüter, B.; Rabeneck, G. *Z. Naturforsch. B* **1973**, *28*, 600.
(51) Lazicki, A.; Hemley, R. J.; Pickett, W. E.; Yoo, C.-S. *Phys. Rev. B* **2010**, *82*, 180102.
(52) Zheng, C.; Hoffmann, R. *Z. Naturforsch. B* **1986**, *41*, 292−320.
(53) Häussermann, U.; Amerioun, S.; Eriksson, L.; Lee, C.-S.; Miller, G. J. *J. Am. Chem. Soc.* **2002**, *124*, 4371−4383.
(54) Zmii, O. F.; Gladyshevskii, E. I. *Crystallogr. Rep.* **1970**, *15*, 939−941.
(55) Wang, F. E. *Metall. Mater. Trans. A* **1979**, *10*, 343−348.
(56) Sevov, S. C.; Corbett, J. D. *J. Solid State Chem.* **1993**, *103*, 114−130.
(57) Hansen, D.; Smith, J. F. *Acta Crystallogr. B* **1968**, *24*, 913−918.
(58) Thurn, H.; Krebs, H. *Acta Crystallogr. B* **1969**, *25*, 125−135.
(59) Guénée, L.; Yvon, K. *J. Alloys Compd.* **2003**, *356*−*357*, 114−119.
(60) Li, Y.; Wu, D.; Li, Z.-R.; Sun, C.-C. *J. Comput. Chem.* **2007**, *28*, 1677−1684.
(61) Labet, V.; Hoffmann, R.; Ashcroft, N. W. *J. Chem. Phys.* **2012**, *136*, 074503.
(62) Becke, A. D.; Edgecombe, K. E. *J. Chem. Phys.* **1990**, *92*, 5397.
(63) Nesper, R.; Wengert, S. *Chem.—Eur. J.* **1997**, *3*, 985−991.
(64) Takemura, K.; Minomura, S.; Shimomura, O. *Phys. Rev. Lett.* **1982**, *49*, 1772−1775.
(65) von Schnering, H. G.; Nesper, R. *Angew. Chem., Int. Ed.* **1987**, *26*, 1059−1080.
(66) Neaton, J. B.; Ashcroft, N. W. *Nature* **1999**, *400*, 141−144.
(67) Ma, Y.; Eremets, M.; Oganov, A. R.; Xie, Y.; Trojan, I.; Medvedev, S.; Lyakhov, A. O.; Valle, M.; Prakapenka, V. *Nature* **2009**, *458*, 182−185.
(68) Martinez-Canales, M.; Pickard, C.; Needs, R. *Phys. Rev. Lett.* **2012**, *108*, 045704.
(69) Henning, R. W.; Corbett, J. D. *Inorg. Chem.* **1999**, *38*, 3883−3888.
(70) Sevov, S. C.; Corbett, J. D. *Z. Anorg. Allg. Chem.* **1993**, *619*, 128−132.
(71) Stöhr, J.; Schäfer, H. *Z. Naturforsch. B* **1979**, *34*, 653.
(72) Stöhr, J.; Müller, W.; Schäfer, H. *Z. Naturforsch. B* **1978**, *33*, 1434−1437.
(73) Naslain, R.; Kasper, J. S. *J. Solid State Chem.* **1970**, *1*, 150−151.